

THERMAL CONDITIONS DURING THE LUNAR BASIN-FORMING EPOCH: INSIGHTS FROM THE NUMERICAL MODELING OF LUNAR BASIN-FORMING IMPACTS R. W. K. Potter¹, G. S. Collins¹, W. S. Kiefer^{2,3}, P. J. McGovern^{2,3}, D. A. Kring^{2,3}, ¹Impacts and Astromaterials Research Centre, Dept. Earth Science and Engineering, Imperial College London, London, SW7 2AZ, UK, ross.potter04@imperial.ac.uk; ²Lunar and Planetary Institute, 3600 Bay Area Boulevard, Houston, TX, USA, 77058, ³NASA Lunar Science Institute

Introduction: Over 50 multi-ring basins have been identified on the Moon [1], with the youngest, Orientale Basin, forming ~ 3.8 Ga. Lunar basins therefore formed within ~ 700 My of the Moon's existence; the majority are thought to have formed during the basin-forming epoch - the Lunar Cataclysm [2] - a spike in the impact bombardment rate ~ 4.1 - 3.9 Ga. The thermal state of the Moon during this basin-forming epoch is unclear, though the Moon is assumed to have been hotter than its present state [3].

Gravity-derived lunar basin structure [4,5] suggests two crustal features are common to lunar basins: (1) a (relatively) thin crustal layer beneath the basin center flanked by (2) a (relatively) thickened annulus (ring) of crustal material. These features are present in all but the oldest pre-Nectarian basins [5]. This implies thermal conditions (and subsequent post-impact processes) early on in the basin-forming epoch were different to those towards the end of the basin-forming epoch.

This work numerically models lunar basin-forming impacts using thermal profiles estimating conditions for a young, warm Moon during the basin-forming epoch. The results of the basin-scale simulations are compared to gravity-derived lunar basin crustal profiles and used to estimate basin features, such as transient crater diameter, for a suite of lunar basins. The simulation results and estimations are then used to suggest whether the investigated thermal profiles are suitable analogs for lunar thermal conditions during the basin-forming epoch.

Methods: Lunar basin numerical modeling was carried out using the two dimensional iSALE hydro-code [6,7] previously used to model large-scale terrestrial impacts such as Chicxulub [8].

The impact target was modeled as an infinite half-space divided into a crustal and mantle layer. A Tillotson equation of state derived for gabbroic anorthosite [9] and an ANEOS-derived equation of state for dunite [10] were used to model the crust and mantle response, respectively, to thermodynamic changes and compressibility. Material strength and thermal parameters for each layer were derived from fits to experimental gabbro and dunite rock strength data [11-14]. Impactor diameter was varied between 40 and 120 km; a constant resolution of 20 cells per projectile radius (CPPR) was used, resulting in cell sizes of 1-3 km. Impact velocity was varied between 10 and 15 km/s.

Thermal profiles (TP) estimating lunar conditions for an early, warm Moon, based on [15] were investigated. TP1 had a near-surface temperature gradient of 34 K/km, with a deep mantle temperature of ~ 1770 K; TP2 had a near-surface temperature gradient of 10 K/km with a deep mantle temperature of ~ 1670 K. Temperatures were bound by the solidus; they never exceeded the ambient melt temperature. An additional thermal profile, TP3, modified from [16], estimating a 0.5 Gy old Moon, was also used (Figure 1). Based on the thermal profiles, self-consistent pressure, density and strength fields were computed. The gravity field was set to a constant value of 1.62 m/s^2 .

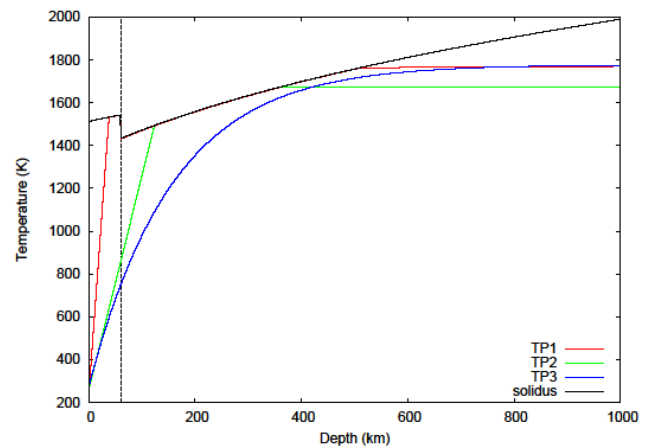


Figure 1. The three temperature profiles investigated. TP1 has near-surface gradient of 34 K/km and a deep mantle temperature of ~ 1770 K. TP2 has a near-surface thermal gradient of 10 K/km with a ~ 1660 K deep mantle temperature. The temperature profiles are bound by the solidus so temperatures never exceed the ambient melt temperature. TP3 is modified from [16] and estimates a 0.5 Gy old Moon.

Results: Due to the high internal temperatures, a far greater volume of melt was produced in the simulations compared to scaling law estimates for comparable lunar impacts [17,18]. In the simulations a significant volume of crustal material was removed forming a thinner post-impact crustal layer than that suggested by gravity-derived crustal profiles [4,5]; some simulations completely removed crustal material from the basin center. Coupled with the greater melt volume, the discrepancy between the simulations and the gravity-derived profiles could be resolved by differentiation of the voluminous melt pools formed in the simulations

into new crustal layers, as suggested by [19] for the South Pole-Aitken Basin-forming impact.

Simulations using TP2 and TP3 were however qualitatively consistent with the location and thickness of the thickened crustal annulus of gravity-derived crustal profiles [4] for a suite of lunar basins covering age groups I1 (Imbrium) to P11 (Smythii). To produce the same crustal annulus radius, greater impact energy was required for impacts using TP3 as it was cooler and stronger than TP2. Impacts into TP1 did not produce qualitatively similar basins to gravity-derived crustal profiles; hot crustal material flowed in towards the basin center smoothing out any topography and crustal thickening created during the initial stages of impact. TP1 therefore appears to be too warm to explain inferred basin structures for this suite of basins.

Assuming differentiation can account for the differences between the simulations and the gravity-derived crustal structure around basin centers, the basins formed in TP2 and TP3 were used to predict features for the suite of lunar basins, including transient crater and apparent basin rim size (Figure 2). By comparison to scaling law estimates and observed basin structure, TP2 appeared to be slightly too warm and weak to produce basins with features similar to those observed, while TP3 appeared to be slightly too cool and strong to produce basins with features similar to those observed.

Discussion: Thermal conditions during the latter stages of the lunar basin-forming epoch can be roughly constrained by mare volcanism; this is thought to have begun ~4 Ga [20] prior to the end of the basin-forming epoch. The mare basalt is a product of ultramafic magmas and is thought to have been sourced from depths between 150 and 400 km [21] suggesting some partial melting within the upper mantle. The upper mantle temperature in TP2 matches the mantle solidus between depths of 150-350 km, while upper mantle temperatures in TP3 approach the mantle solidus between depths of 300-500 km. Therefore a thermal profile with a similar near-surface thermal gradient to TP2 and TP3 (10 K/km) and a deep mantle temperature in between those of TP2 and TP3 could possibly produce basins with features similar to those observed and inferred and provide a reasonable estimate for thermal conditions during the latter stages of the basin-forming epoch.

Acknowledgements: We are grateful to Boris Ivanov, Jay Melosh, Kai Wünnemann and Dirk Elbeshausen for their work in the development of iSALE. RWKP and GSC were funded by NERC.

References: [1] Potter, R. W. K. et al (2011) *LPSC XLII*, #1452 [2] Tera, F. et al (1974) *EPSL*, 22, 1-21 [3] Shearer, C. K. et al (2006) *Rev. Min. Geochem.*, 60,

365-518 [4] Wieczorek, M. A. & Phillips, R. J. (1999) *Icarus*, 139, 246-259 [5] Hikida, H. & Wieczorek, M. A. (2007) *Icarus*, 192, 150-166 [6] Amsden, A. A. et al (1980) *Los Alamos National Laboratory Report LA-8095* [7] Collins, G. S. et al. (2004) *MAPS*, 39, 217-231 [8] Collins, G. S. et al (2008) *EPSL*, 270, 221-230 [9] O'Keefe, J. D. & Ahrens, T. J. (1982) *GSA Spec. Pap.* 190 [10] Benz, W. et al (1989) *Icarus*, 81, 113-131 [11] Azmon, E. (1967) *NSL* 67-224 [12] Stesky, R. M. et al (1974) *Tectonophys.*, 23, 177-203 [13] Shimada, M. et al (1983) *Tectonophys.*, 96, 159-192 [14] Ismail, I. A. H. & Murrell, S. A. F. (1990) *Tectonophys.*, 175, 237-248 [15] Potter, R. W. K. et al (2011) Submitted to *Icarus* [16] Spohn, T. et al (2001) *Icarus*, 149, 54-65 [17] Cintala, M. J. & Grieve, R. A. F. (1998) *MAPS*, 33, 889-912 [18] Wünnemann, K. et al (2008) *EPSL*, 269, 529-538 [19] Morrison, D. A. (1998) *LPSC XXIX*, #1657 [20] Hiesinger, H. et al (2011) *GSA Spec. Pap.* 477 [21] Heiken, G. H. et al (1991) *Lunar sourcebook: A user's guide to the Moon*, Cambridge Uni. Press, New York [22] Pike, R. J. & Spudis, P. D. (1987) *Earth, Moon, Planets*, 39, 129-194 [23] Spudis, P. D. (1993) *The geology of multi-ring impact basins*, Cambridge University Press, Cambridge [24] Spudis, P. D. & Adkins, C. D. (1996) *LPSC XXVII*, #1627 [25] Croft, S. K. (1985) *Proc. 15th LPSC*, C828-C842

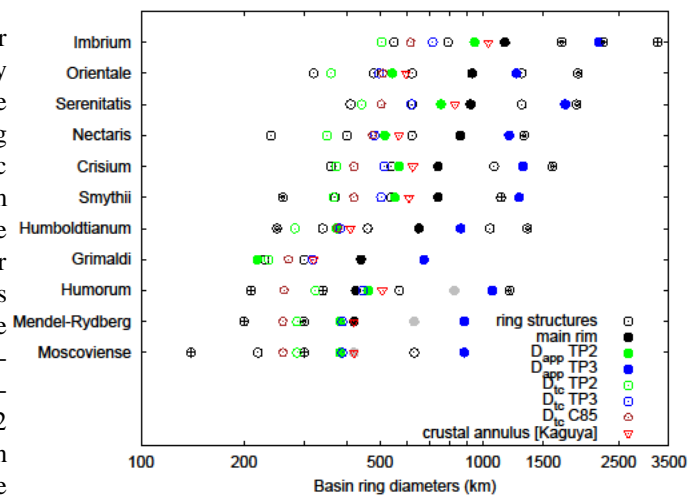


Figure 2. Structural features for a suite of 11 lunar basins. Data includes: ring diameters [22] (open black circles represent definite ring structures; partially filled circles represent uncertain ring structures), main rim diameter estimates [23] (black circles), alternative basin rim diameter estimates [24] (gray circles), transient crater diameter estimates from [25] (C85) and this study, and crustal annulus diameter estimates (Kaguya data). Data from this study for thermal profiles TP2 (green circles) and TP3 (blue circles) plot either side of scaling estimates and observations for a given basin feature. Dtc is the transient crater diameter; Dapp is the apparent basin rim diameter.